Design, Development, and Control of a Hand/Wrist Exoskeleton for Rehabilitation and Training

Mihai Dragusanu, *Graduate Student Member, IEEE*, Muhammad Zubair Iqbal, *Member, IEEE*, Tommaso Lisini Baldi, *Member, IEEE*, Domenico Prattichizzo, *Fellow, IEEE*, and Monica Malvezzi, *Member, IEEE*

***Abstract*—Robotic devices for rehabilitation and training is a promising and challenging research topic with a potentially huge social impact. The availability of tools for autonomously performing physiotherapy exercises increases their efficiency, provides supplementary information about results and progress, reduces physiotherapists' efforts and the need of their physical presence during exercise sessions, and encourages autonomy and independence in people with disabilities. Nevertheless, supportive technologies developed without the inputs and feedback of the end-user throughout the design process are less likely to be adopted for their intended purpose and use case. In this article, we propose a modular hand/wrist exoskeleton that actuates the wrist flexion/extension and adduction/abduction motions and hand fingers flexion/extension motions. It is designed to be wearable and easy to control and manage and can be used by the patient in collaboration with the physiotherapist or autonomously. A user-centered design perspective has been employed in all the design and development phases. This article introduces the main features of the device and presents some tests conducted with a user having limited hand and wrist mobility.**

***Index Terms*—Exoskeletons, Rehabilitation robotics, Wearable robots.**

I. Introduction

NOWADAYS, most of the people are living a longer and healthier life than in the past. The mean age of the population increases and, as a consequence, the overall social impact of chronic diseases related to the musculoskeletal and nervous systems becomes more important. The World Health Organization statistics show that nearly one billion people worldwide are suffering due to the neurological and musculoskeletal diseases [1]. On the other hand, the spreading of technology in everyday life is playing an important role in preserving and guaranteeing a high quality of life also in the presence of temporary and/or permanent diseases [2].

At the beginning of 2020, COVID-19 pandemic dramatically modified most of our habits, including medical and rehabilitation practices, that necessarily had to be delivered remotely through audiovisual technology. Orthopedic and rehabilitation also shifted from face-to-face visits to audiovisual-guided sessions. In the immediate future, telerehabilitation could further spread and become more common. Despite some limitations, there are evident advantages in distance rehabilitation, whether synchronous (real-time) or asynchronous (store-and-forward). The implementation of telehealth rehabilitation, which was initially considered difficult or even impossible, has now been forced to be utilized widely [3].

In particular, robot-augmented therapy is a clinically verified path to improve rehabilitation outcomes in several neuromuscular disorders, such as cerebrovascular and spinal cord injuries [4]. Technology advancements in the medical and assistive fields allow people with disabilities and diseases to have a life that in many cases is almost completely autonomous. Devices and supports can help in the autonomy of activities of daily living (ADLs), such as in communication, study, learning, and more, in general, in the whole process of integration. In this context, the use of robotic rehabilitation aids has shown great potential since they combine the high intensity, the long duration interventions needed for regaining motor function, and quantitative metrics for assessing therapeutic outcomes [5].

The capacity of performing precise and repeatable therapeutic exercises, reducing the physiotherapists' physical burden, embedding virtual reality systems, collecting quantitative data that can be used to optimize therapy sessions, and assess patient outcomes are the main advantages offered by rehabilitation robotics.

Many researchers focused on developing devices designed to retrain impaired upper limbs [6], [7]. Regaining the "pick and place" and "grasping" abilities allows patients to perform the majority of ADLs, retrieving both functional improvements and independence. Therefore, successful upper arm therapy requires to focus not only on the arm but also on the wrist and the hand. Indeed, hand therapy via exoskeletons and, more in general, rehabilitation robotics has received growing attention in the last decades. Lately, a number of robots have been developed to provide upper-limb motor therapy. All these devices have similar

Manuscript received August 4, 2021; revised December 6, 2021 and March 22, 2022; accepted April 19, 2022. Date of publication May 20, 2022; date of current version June 7, 2022. This article was recommended for publication by Associate Editor N. Vitiello and Editor M. Yim upon evaluation of the reviewers' comments.. *(Corresponding author: Monica Malvezzi.)*

Mihai Dragusanu, Muhammad Zubair Iqbal, Tommaso Lisini Baldi, and Monica Malvezzi are with the Department of Information Engineering and Mathematics, University of Siena, 53100 Siena, Italy (e-mail: dragusanu@diism.unisi.it; muhammadzubair.iq@student.unisi.it; lisini@diism.unisi.it; malvezzi@diism.unisi.it).

Domenico Prattichizzo is with the Department of Information Engineering and Mathematics, University of Siena, 53100 Siena, Italy, and also with the Department of Humanoids and Human Centered Mechatronics, Istituto Italiano di Tecnologia, 16163 Genova, Italy (e-mail: prattichizzo@ing.unisi.it).

Color versions of one or more figures in this article are available at https://doi.org/10.1109/TRO.2022.3172510.

Digital Object Identifier 10.1109/TRO.2022.3172510

goals: to develop a training platform that helps patients regain hand range of motion and the ability to grasp objects, ultimately allowing the impaired hand to partake in ADLs.

These devices widely differ in terms of cost, design philosophy, actuated degrees of freedom (DOFs), and range of motion. In what follows, we retrace the most paradigmatic examples of exoskeletons relevant to the topic.

Dovat *et al.* [8] present HandCARE, an exoskeleton for the hand that uses cable loops attached to the ends of each digit. A motor and pulley system applies forces to the digits, while a clutch design allows individual actuation of the fingers and thumb. The Rutgers Hand Master II proposed in [9] is a force-feedback glove powered by pneumatic pistons positioned in the palm of the hand.

A different design philosophy was exploited by Lambercy *et al.* in [10], where a parallelogram structure that presents two movable surfaces squeezed by the subject was presented. The hand module developed in [11] uses a double crank and slider mechanism driven by an electric motor. The operation of the motor controls the radius of the cylinder and guides grasping motions. A common disadvantage of the aforementioned devices is the limited control of the proximal joints of the fingers, which may lead to physiologically inaccurate joint kinematics. In [12], the kinematic synthesis of a hand finger exoskeleton based on a parallel mechanism is presented as the base stem for developing a robotic-assistive device for hand opening disabilities. Control strategies for this exoskeleton based on sEMG systems are presented in [13] and [14].

Cable-driven devices have been developed that allow for individual control of the fingers and thumb with pulley systems that rest on the dorsal surface of the hand [15], [16]. Bowden cables allow the motors to be remotely located reducing the overall weight so that these devices can be used in conjunction with arm movements. In [17], tendons are replaced with an air chamber and channels that run along the palmar side of the hand digits. An electropneumatic servovalve is used to regulate air pressure to provide assistance in digit extension. In [18], the hand wrist assistive rehabilitation device is presented. The exoskeleton directly controls finger rotation about the metacarpophalangeal (MCP) joint, thumb abduction/adduction, and wrist extension/flexion. The hand mentor (Kinetic Muscles, Inc., Tempe, AZ, USA) is a commercially available exoskeleton device that uses an artificial muscle to simultaneously extend and flex the fingers and wrist but the thumb is not actuated [19]. Finally, a system based on the three-dimensional (3-D) printing technology for assisting stroke patients to perform rehabilitation exercises was developed in [20]. Recently, a wearable soft exoskeleton for hand rehabilitation has been presented in [21], while in [22], a Bowden-cable-based bidirectional remote actuation system is presented, featuring high power-to-mass and power-to-volume ratios, easily accessible components, and compact mechanical design. An interested reader is referred to [23]–[25] for a more comprehensive review on hand exoskeletons.

Considering also the wrist, Krebs *et al.* [26] presented a robot for wrist rehabilitation designed to provide three rotational DOFs. Similarly, Gupta *et al.* [27] present the RiceWrist. It is a high fidelity 4 DOFs wrist exoskeleton for training and rehabilitation purposes. The RiceWrist is intended to provide kinesthetic feedback during the training of motor skills or rehabilitation of reaching movement. A soft wrist orthosis exoskeleton, which is able to actively assist users in all DOFs, is detailed in [28]. Wrist actuation systems are often integrated in upper-limb exoskeletons, including elbow and shoulder actuation. For a more comprehensive review, the interested reader could refer to [29].

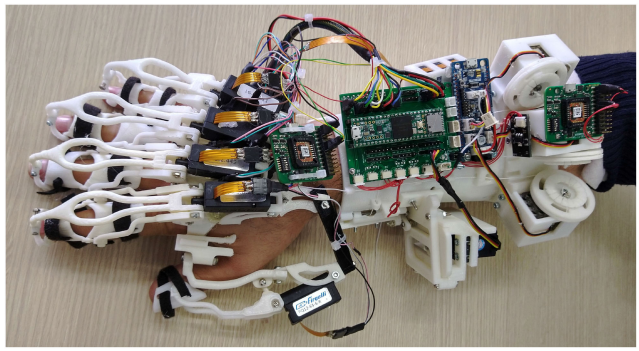

Fig. 1. Prototype of the hand/wrist exoskeleton for rehabilitation and training worn by a user.

Notwithstanding all the technological developments just described and the presented evidence of clinical effectiveness of robotic technologies for upper-limb neurorehabilitation, there are still some limits to their diffusion [30]. Technological and economic barriers together with communication biases between the producers of the technologies are still open issues.

Besides the technological and economical barriers above mentioned, it is worth to observe that supportive and rehabilitative technologies that are developed without the input of the end-user throughout the design process or without knowledge of how the technology will be used are less likely to be adopted for its intended purpose and use case. This approaches the risk that the developed technology may be designed to meet requirements that are irrelevant to the intended user and use case. Rather, the design of technology has to meet the needs of the user engaged in the relevant activity across necessary contexts, including the utility needs, the usability, occupational, and social requirements factors [31]. Rehabilitation and assistive robotics, in particular, ought to be accepted and adopted into everyday practice by the users. To meet this goal, it is necessary to discern user's specific needs (quality of life, the feeling of being in control, dignity, and independence) as well as deal with her/his perspective fears and expectations. It has been argued that involving the intended users in a participatory design process might help overcome conflicting values and expectations of developers and end-users [32] and contribute to filling the gap between device developers and end-users.

In this article, we propose an exoskeleton for hand and wrist motion assessment and training (see Fig. 1) that has been designed to be easily and independently wearable, easy to control and manage, modular, and versatile. The proposed device can be used by the patient in collaboration with the physiotherapist or autonomously and is composed of two independent and modular

elements: the wrist actuation and the hand actuation systems. To the best of our knowledge, the proposed device represents the first attempt to realize a wearable hand/wrist exoskeleton able to record and play back motions and, at the same time, store data for further analyses.

The rest of this article is organized as follows. In Section II, the main design requirements for the proposed wrist/hand exoskeleton are introduced and discussed. Section III describes the proposed devices, focusing, in particular, on its hardware and actuation part. Section IV focuses on the device tracking system, control, and user interface. In Section V, the results of a set of tests are presented and discussed. Finally, Section VI concludes the work.

II. Design Requirements

The goal of this article is the development of an actuated hand/wrist exoskeleton suitable for upper-limb rehabilitation and training, usable both in the clinic/rehabilitation center and at home for people with long-term impairments. As introduced in the previous section, the design process was user-centered. A potential user was involved from the first phases of the device. Starting from his needs, an appropriate set of design requirements was defined. The design process was aimed at fulfilling the defined requirements to the highest possible extent; furthermore, the user was also involved in the design and development phases; his feedback and suggestions were taken into account and the requirements were accordingly adjusted. This section presents the main requirements that guided the design of the device.

A. Identification of the Target Application

The definition of a comprehensive set of design guidelines for assistive and rehabilitation hand and upper-limb exoskeletons is impossible since the impairments and disabilities (e.g., stroke, muscular dystrophy, brachial plexus injury, SCI, etc.) involve high variability in the available range of motion, muscle tone, joint stiffness, etc. Furthermore, even for the same disease, such characteristics vary according to severity level and time since injury, subject's age, etc. [33]. In [34], a study for identifying design criteria for the development of an assistive powered hand exoskeleton is presented. The study was based on structured interviews with clinicians and patients with hand impairment and also with some measures of patient's hand capabilities. Such a study reported a considerable variety in the needs and expectations.

The device developed in this article is, therefore, designed for a specific application, namely, as a rehabilitation and training for a subject with low residual force, low active control of the hand and the wrist, low spasticity, and low muscle tone. We developed the device for the needs and requirements of a representative user, but as we will detail in the following sections, the modular structure of the proposed solution makes it adaptable to different subjects and different needs.

B. Mechanical Requirements

1) Wrist Module: Wrist articulation allows the following motions: 1) flexion/extension, 2) radial deviation or adduction and ulna deviation or abduction3) pronation/supination. Starting from an initial reference configuration, typical values for the amplitude of both flexion and extension motions are 85° and 40°–45° for the adduction, and less than 20° for the abduction. Pronation/supination motion has not been considered in this work since it involves the whole forearm and would need the device to be extended at least up to the elbow.

The wrist module is requested to support the patient in the execution of the following exercises: 1) full or partial flexion/extension with predefined profiles or guided by the physiotherapist with an amplitude that can be selected in the physiological range previously mentioned; 2) full or partial abduction/adduction with predefined profiles or guided by the physiotherapist with an amplitude that can be selected in the physiological range previously mentioned; 3) coupled flexion/extension and abduction/adduction guided or prerecorded by the physiotherapist. In the guided exercises, both the amplitude and the speed can be varied.

2) Hand Module: The human hand has a complex mechanical structure that can be represented with a 30 DoFs system [35]. Each finger can be represented as a kinematic chain, with one universal joint (two intersecting, orthogonal revolute joints) representing the MCP joint and two hinges for the proximal (PIP) and distal (DIP) interphalangeal (IP) joints. If the hand is not affected by particular pathologies, we can assume that the rotation axes of PIP, DIP, and the flexion/extension of one of the MCP are parallel. Furthermore, the thumb has a more complex structure with at least 5 DoFs: 2 DoFs in trapeziometacarpal joint, 2 DoFs in MCP joint, and 1 DoF in IP joint. In this work, we reproduced the opening/closing motion of the hand, which corresponds to a finger motion that includes mainly an extension/flexion motion and a more limited adduction/abduction motion. In order to keep as limited as possible the complexity of the exoskeleton and the number of actuators, only the flexion/extension motion is actuated, while the adduction/abduction is left unconstrained.

The hand exoskeleton has two coupled bending DOFs to exercise the MCP and PIP joints of the finger. In tripod grasping, typically, MPC, PIP, and DIP flexion angles are around 46°, 48°, and 12° for the index, and 46°, 54°, and 12° for the middle finger [36], [37]. Regarding the speed, according to [38], physiotherapists suggest a speed lower than 20 s for a complete flexion/extension cycle of a finger joint and of course hyperextension of all these joints should be carefully avoided. Concerning the required forces, Li *et al.* [37] underline that in grasp tasks, the forces required are typically below 20 N. In summary, the hand module of the device is required to support the user in realizing flexion/extension motions of all the fingers with an amplitude that can be varied in the whole physiological extension previously summarized. The fingers are requested to be controlled both independently and in a coordinated way. Adduction/abduction motion of the fingers is not controlled by the exoskeleton and neither constrained by its mechanical structure.

C. Requirements for Wearability and Adaptability

Preliminary studies and first prototypes of the device have been introduced in [39] for the wrist and in [40] for the hand.

Initial users' feedback revealed that one of the main limits of these prototypes was that it was impossible for the user to wear them autonomously. One of the main requirements to be addressed is, therefore, providing the possibility also for users with limited motion capabilities of the upper limb to wear and use it. Another important aspect that has been considered is the adaptability of the device to user's specific characteristics (i.e., anthropometric measurements). In this context, the parts of the device in contact with the user's hand, finger, and forearm have been developed with a parametric approach that allows to automatically adapt them to different users by means of a limited number of measures that can be easily obtained. Regarding the hand part, to limit as much as any possible interference during ADLs, the mechanical transmission system has to be constrained to be on the back of the fingers and the palm; the width of the finger modules should not exceed too much of the finger width. The weight of the exoskeleton should be as light as possible and the inertia should be distributed so as not to fatigue the patient.

The solution presented in this work includes two modules: one for the hand and one for the wrist. Hand modulus can furthermore be divided into finger submodules since it was developed for a target user that needs to train both wrist and hand motions. However, the structure and control have been developed so that each module can be used and controlled independently. For example, if the user wants to train only the wrist, it is not necessary that she/he also wears the hand part.

D. Requirements for Control

The device can be used for executing predefined exercises, e.g., wrist flexion/extension or adduction/abduction and hand opening/closure with predefined profiles (e.g., sinusoidal, trapezoidal, etc.) in which the user can define a limited number of parameters (e.g., amplitude, time–frequency, duration). Another feature that the user required was the possibility of recording an exercise guided by a physiotherapist, store it, and replay it at any time he needs it, for example, at home, autonomously. Since the device has a modular structure, the developed control system and GUI should allow to manage and control both the whole system and every single module independently.

III. Device Description

As previously introduced, the whole device comprises two modules: the wrist module and the hand module. The proposed solution for the wrist consists of a tendon actuated system with two main elements worn on the hand and on the forearm, respectively. Opening/closing motion of the hand is actuated by means of five finger modules with one actuator per module. The CAD representations of the hand and wrist modules are shown in Fig. 2. In what follows, before tackling the algorithmic development and experimental evaluation, we describe in detail all the mechanical parts comprising the exoskeleton.

A. Wrist Actuation

The wrist module was built up on a previous preliminary prototype [39]. Although the above-mentioned system was simple and low cost, it was not suitable for users with limited motion capabilities, and the Velcro-based closure system resulted in undesired (or infeasible) relative motions between the device and the forearm.

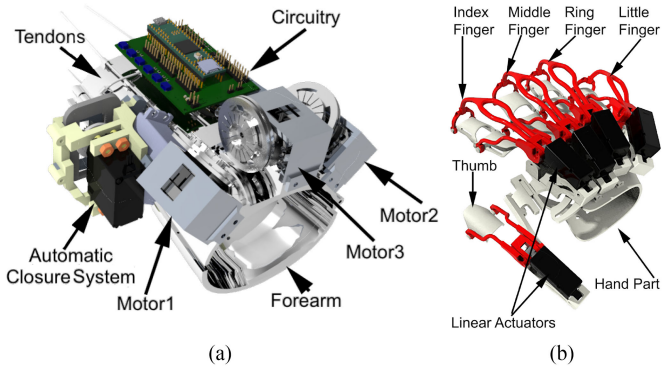

Fig. 2. Exoskeleton prototype CAD renderings. (a) Wrist module. (b) Hand module.

In the version here presented, the wrist module has been significantly improved, in particular, the part connected to the forearm. The most relevant upgrade is represented by an automatic closure system, designed for increasing the wearability.[1] The complete forearm CAD model is shown in Fig. 2(a). The support has been modeled with Autodesk Fusion360 software in accordance with the user's specific anatomical characteristics. Moreover, the forearm support has been modeled with a parametric approach that allows to easily adapt it to different users, in particular, on the basis of 1) forearm circumference close to the wrist; 2) forearm circumference close to the elbow; and 3) distance between the wrist and the elbow. Also, the 3-D CAD model of the support on the back of the hand can be adapted to different users on the basis of the palm width close to finger MPC joints and palm length (distance between finger MPC joints and wrist). The part of the wrist actuation system connected to the hand, visible in Fig. 2(b), has been modeled in accordance with user's specific anatomical characteristics and represents the support for the hand actuation system. More details on this part are provided in Section III-B.

The structural parts of the wrist module, both on the hand and on the forearm, have been realized in acrylonitrile butadiene styrene (ABS) material through the fused deposition modeling technology.

Regarding wrist joint actuation, the design of this part has been completely redesigned to make it more wearable and fitting to the arm.

User's wrist movement during exercise execution is guided and supported by a 3 DoFs tendon system actuated by three servo motors (Dynamixel XL-320). Two tendons are connected to the upper part of the hand and are used for controlling the extension motion; the corresponding motors are indicated in the following with *Motor1* and *Motor2*. The third tendon is connected to the hand palm and is actuated to control the downward (flexion) motion; its motor is indicated in the following with *Motor3*.

[1]A short video of the automatic closure system is available at [Online]. Available: http://sirslab.dii.unisi.it/exoskeleton/closureSystem.mp4

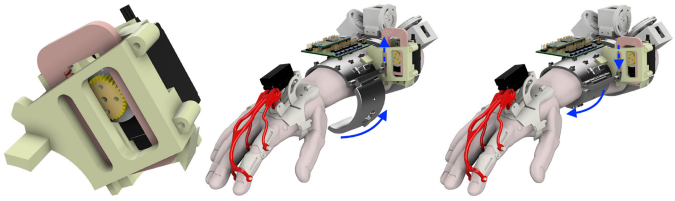

Fig. 3. Exoskeleton rendering highlighting the automatic closure mechanism. (a) Detail of the rack and pinion mechanism used for ensuring a tight closure and allowing batteries to last longer. (b) Open configuration. (c) Close configuration.

Rotation of *Motor1* and *Motor2* along the same directions and rotation of *Motor3* along the opposite direction realize the actuation of the flexion/extension motion. Rotation of *Motor1* and *Motor2* along the opposite directions realizes the actuation of the radial/ulnar deviations. As anticipated in Section II, wrist pronation and supination motions are not activated.

The position of the actuators on the forearm and tendon routing was selected by taking into account that flexion motion is typically easier than extension for a user with low residual force and low muscle tone as the one that represents the target application of this work (see Section II) because of the contribution of the hand weight in standard exercises where the palm side of the hand is facing down. Therefore, for positioning tendons and actuators on the forearm, we assumed that the effort necessary for the extension is higher than for the flexion. Furthermore, pulleys connected to motor shafts have been redesigned with respect to [41]. The pulley diameter has been reduced to take up less space while maintaining the desired range of motion. Compared to the previous version, an external support has been added with a thread fixing system designed in such a way that it can wrap the excess wire length allowing to adjust the length of the tendon according to the anatomical dimensions of the hand/forearm for each user. In addition, the tendon routing has been realized to avoid the tendon getting out of the pulley during the exercises.

One of the novelties introduced in this work is the automatic closure system of the forearm module, needed by the user to easily and autonomously wear it. The assembly shown in Fig. 3(a) is connected to the lower part of the forearm support. As the motor rotates the pinion, the rack translates, and as a result, the lower part of the forearm support rotates to wrap around the arm. This system allows holding the complete forearm assembly firmly around the arm; furthermore, since the rack and pinion structure is not easy to drive back without actuating the servo, keeping the motor active all the time is not necessary. Broadly speaking, automatic closure motors work only during the opening/closure phases when the exoskeleton is worn by the user; this feature allows to save battery lifetime with respect to other solutions. The user can control the opening and closure of the forearm fastening mechanism from the software graphical user interface (GUI) that has been developed to control the exoskeleton and that will be detailed in the following sections. The developed system ensures a comfortable device opening and closure that can be autonomously controlled by the user. The rack and pinion mechanism is actuated by a servo motor (HS-422, Hitec RCD, Inc., USA). The pinion gear driving the rack is connected directly to the output shaft of the motors. The pinion gear is designed to provide a rack stroke suitable for device closure and to provide enough strength to withstand the torque applied by the motor. The maximum rotation range of the motor is limited in the range $10°$–$170°$, the corresponding rack stroke is 20 mm. The mechanism is depicted in Fig. 3, in particular, (b) and (c) show the whole exoskeleton rendering with the automatic closure mechanism in the open and close configurations, respectively, while (a) shows a close-up of the rack-pinion mechanism controlling it.[2]

In order to place and align the wrist module, the tendon system helps the user in wearing it easily (since the tendons are flexible) and correctly. Two tendons are connected to the dorsal part of the hand module, while the third tendon, routed through the closure mechanism, is connected to the palm of the hand module. This helps the user to insert the hand into the hand-exoskeleton module by keeping in mind that two tendons, the lateral ones on the wrist exoskeleton, must remain above the hand, while the central one must go under the hand. The basic idea for using the wrist exoskeleton that uses a tendon actuation is to always keep the tendons tight. Indeed, as soon as the user feels a comfortable position with the device worn, she/he or the physiotherapist can use the GUI to block the exoskeleton and then set it in the initial position, i.e., the automatic closure mechanism is activated and the tendons are pulled until they are tight. It is worth to notice that since the wrist actuation system is tendon-based and inherently underactuated, it is adaptable to different user's characteristics and can compensate for misalignment or partially incorrect positioning.

B. Hand Actuation

The hand actuation system is composed of five modules, one per finger, that can be jointly or independently controllable. The hand exoskeleton module, therefore, consists of two main parts: the support for the finger modules, where the tendons of the wrist exoskeleton are also connected, and the finger modules. The hand exoskeleton can be worn by inserting the hand inside this support that has been designed taking into account the user's hand shape and dimensions. Its internal part is lined with spongy material, while the external part is made of ABS. Two solutions for these parts have been developed. The first solution consists of two parts, i.e., one for the dorsal part of the hand and the other for the palm, and these are fixed to the user's hand through a Velcro strap. The second solution is made in a single piece, avoiding the use of the Velcro strap and making it more resistant to the forces applied by the wrist actuation system. The second version was better evaluated by the user. In the upper part of the support, there is a horizontal slot where the individual finger modules can be fixed, while the bottom part is designed in such a way as to keep the palm uncovered. In both parts, a set of holes is realized in order to connect the tendons of the wrist module.

The position of the finger modules can be adjusted in the lateral direction, thanks to the horizontal slot on the hand support,

[2]A short video showing the working principle is available at [Online]. Available: http://sirslab.dii.unisi.it/exoskeleton/latch.mp4

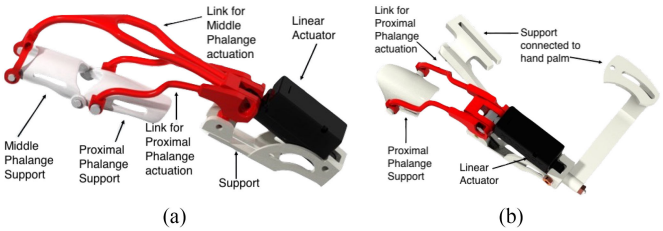

Fig. 4. Hand module. (a) CAD model of single-finger part. (b) CAD model of thumb part.

TABLE I
MAIN CHARACTERISTICS OF THE LA

Technical Features	
Mass	15 g
Max. force (lifted)	45 N
Stroke	20 mm
Feedback potentiometer	5 kΩ
Stall current	550 mA @ 6V
Max duty cycle	20 %
Max speed (no load)	15 mm/s
Feedback potentiometer resolution	0.5 mm

and can be moved back and forth, thanks to the motor support made with an extrusion along its base.

The modules for the index, middle, ring, and little fingers have the same mechanical structure with different dimensions, while the thumb module has a different mechanism due to its particular kinematic structure [42]. In Fig. 4(a) and (b), we report the rendered CAD models of the fingers and thumb, respectively. In exoskeletons, actuators are the elements that usually have the highest impact on the overall device weight and encumbrance. Thus, to reduce the inertial loads that may fatigue the user, we positioned the actuators on the back of the hand and the motion is transmitted to the joints through a mechanical linkage systems, as shown in Fig. 4(a) and (b).

One linear actuator (LA) PQ12-63-6-R from Actuonix has been used for each finger. It moves both the proximal and intermediate phalanges, and it is able to apply bidirectional forces. The main characteristics of this LA are summarized in Table I.

The mechanical transmission was developed to implement the concept of postural synergies, introduced by the neuroscientific studies presented in [43]. In particular, the position and dimension of the exoskeleton linkages have been defined to reproduce the first postural synergy on each finger. At the same time, in the hand module, we maintained the fingers independent. In other words, for each finger, the transmission mechanism is designed to replicate the same coordination between the PIP and intermediate IP joints observed in the first postural synergy, but each finger can be independently controlled. This choice allowed us to use one actuator per finger while maintaining good versatility, thanks to the independence between the fingers. Automatic synthesis procedures allow to properly define linkage

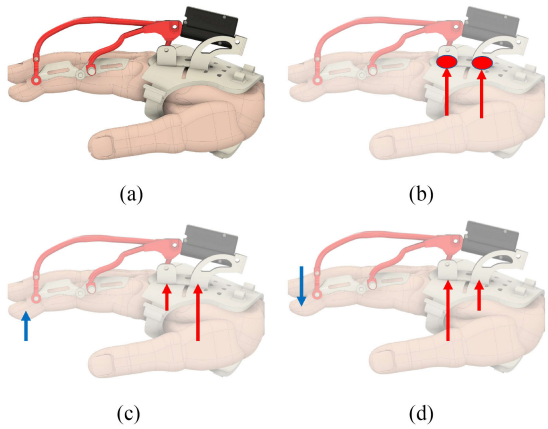

Fig. 5. (a) CAD rendering representing the finger module worn by the user. (b) Red dots indicate where FSR sensors are positioned; when no external forces are applied by the actuator or externally to the finger, we assume that the reaction forces between the actuator support and the hand back support, measured by the FSR sensors, are constant and equal. (c) When a force is applied to the fingertip to open the finger (extension), the reaction forces on the support are different, and the one farther from the MPC joint increases. (d) When a force is applied to the fingertip to close the finger (flexion), the reaction force on the support closer to the MPC increases.

dimensions on the basis of the user's hand anthropometric measurements (lengths of the phalanges), as detailed in [40]. The kinematic structure of the finger actuation system and, in particular, the mechanism for coupling the MCP and PIP joints has been changed with respect to the one presented in [40] to improve its lightness and adaptability to user's fingers. The details of the design process that led to the current version of the finger modules have not been reported in this article for the sake of brevity; the interested reader could refer to a recent publication in which the finger module mechanical design has been detailed [44].

LAs, due to their nature, are not back drivable; this means that a physiotherapist cannot freely open or close the hand (i.e., flex or extend the fingers) while the patient wears the hand exoskeleton. To overcome this limitation, we provided the exoskeleton with a system for active tracking and cancellation of the forces exerted by the hand or by the physiotherapist on the exoskeleton. The idea consists of estimating the force applied on the fingertip, for example, when the physiotherapist opens or closes the hand, by measuring the reaction force on the support connecting the exoskeleton to the hand back component. For this purpose, two force-sensitive resistors (FSRs) are installed under the LA base; the forces measured by the FSR sensors are used to define a reference position signal to move the LA back and forth when the physiotherapist applies forces on the fingertip, as shown in Fig. 5.

It is worth noticing that a force applied to the fingertip can be estimated by measuring the reaction force and moment on the point in which the actuator is connected to the hand back, as it can be verified with a quasi-static analysis of the system composed of the finger and the exoskeleton. An estimation of the reaction force can also be obtained with two force sensors, as shown in Fig. 5. This possibility is also evident by observing the results of the stationary structural analysis based on the finite

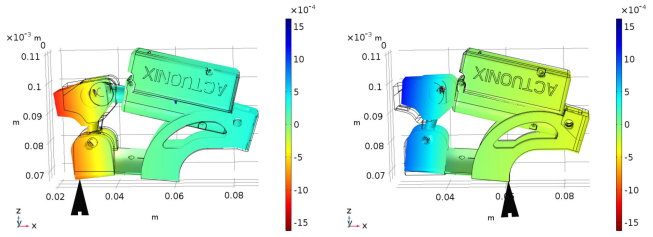

Fig. 6. Results of FEM analysis on finger module support to evaluate force distribution generated by physiotherapist pulling and pushing action on the fingertip. (a) Result generated by a pulling force applied on the fingertip of the index finger. (b) Result generated by a pushing force applied on the middle finger pulp. Black arrows represent the placement of pressure sensors.

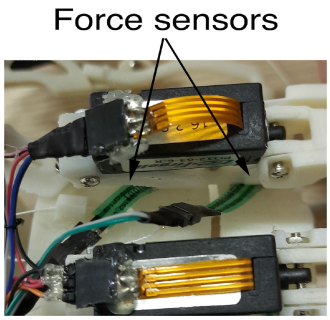

Fig. 7. FSR sensors positioning in the index finger module.

element method (FEM) on the CAD model of one of the finger modules, represented in Fig. 6(a), in which an external force with magnitude of 5 N in opposite direction is applied on the fingertip. In particular, Fig. 6 displays the results in terms of displacement. The aim of this structural analysis was to verify the overall exoskeleton stress/deformation distribution when an external force is applied, but the outcomes of the analyses highlighted how the physiotherapist force is transmitted through the different elements of the exoskeleton, and in detail, how it can be measured with force sensors on the back part of the hand palm (see Fig. 6). We exploited this result for controlling the LA in both directions, following the desired motion guided by the physiotherapist. For each finger, two small FSR sensors (Ohmite FSR04, active area diameter $5.60\,\mathrm{mm}$) are placed at the points identified with the FEM analysis between the motor support and the hand shell. This type of sensor exhibits a decrease in electrical resistance with an increase in force applied to its surface. More specifically, the chosen sensor can measure normal forces in the range 0.2–50 N, presents a long-term drift lower than 2%, and repeatability of 2% (with an applied force of 10 N). The range of measurable forces, the reliability, and the small dimensions of this sensor are compatible with the requirements for controlling the LA in the backward mode. A detailed prototype view showing the embedded sensors is reported in Fig. 7. Considering a single finger, ideally, when no forces are applied on the fingertip, the output from the sensors is the same. On the contrary, pushing and pulling forces applied by the physiotherapist on the distal phalanx generate different compressions of the sensors from which an output proportional

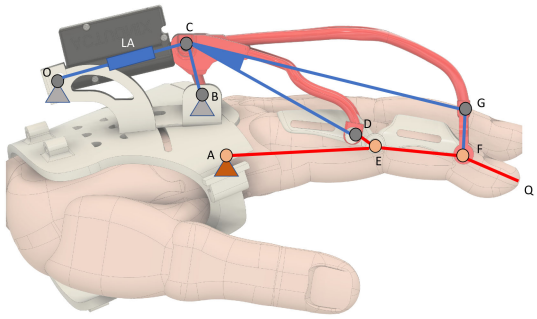

Fig. 8. Kinematics model of the finger exoskeleton worn by a user.

to the force can be estimated. Thus, a PD controller has been realized that seeks to keep the forces measured by the sensors to zero. In this way, the fingers gently follow the desired motion in both directions. The position of each joint can be estimated from the actuator stroke, thanks to the kinematics structure of the mechanism. This type of control that aims at minimizing the difference between the forces detected by the FSR sensors is sufficiently insensitive to errors due to device misalignment. Furthermore, a calibration procedure is available if the force offset induced by undesired sources cannot be neglected.

As a preliminary experimental test devoted to device kinematic validation, we evaluated the capability of the proposed fingertip actuation mechanism in following the first synergy trajectory. The kinematic structure of the exoskeleton worn by a user is shown in Fig. 8. The LA is connected to the hand back support by means of a hinge joint indicated with O and by means of the link BC. Through the hinge joint indicated with C, the actuator moves the main element of the exoskeleton (two links rigidly connected). The first one, indicated with CD, is connected to the link fixed on the proximal phalanx, while the second one, indicated with CG, is connected to the link GF and then to the link EF fixed on the middle phalanx. The main difference between this structure and most of the ones available in the literature is that when the exoskeleton is not worn on the finger, it has 3-DoFs; therefore, it is underactuated, whereas when it is worn on the finger, its biomechanical structure closes the mechanism and reduces the number of DoFs to 1. In this way, the remote center of motion (RCM) for the MCP joint is no more necessary, leading to a significant simplification of the mechanical structure. While simplifying the mechanical structure in the synthesis of the finger exoskeleton, an approach similar to the one described in [40] and based on the reproduction of the first postural synergy of the human hand has been adopted.

First, a kinematic simulation was conducted for each finger; in Fig. 9, we report a plot of the index finger for different values of the MCP rotation angle varying from 1° to 45°. Then, once the theoretical feasibility was assessed, we validated the accuracy of the prototype by means of an optical tracking system. We exploited a Vicon tracking system consisting of 10 Bonita cameras and $6.4\,\mathrm{mm}$ retroreflective markers to track the motion of the exoskeleton. For the sake of comparison, in Fig. 10, we report a representative trajectory obtained by the index finger only.

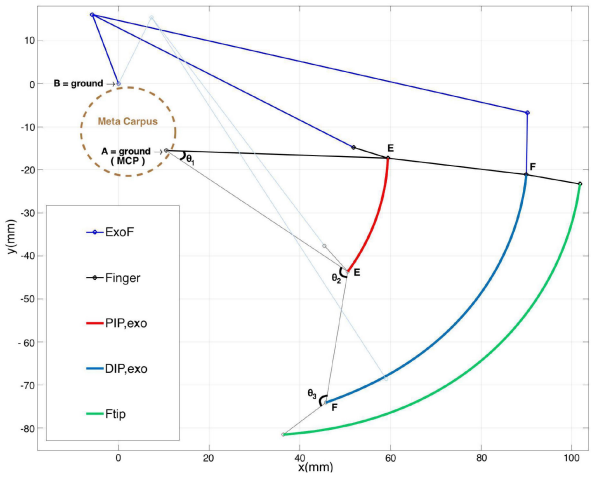

Fig. 9. Kinematic simulation of the index finger module for different values of the MCP rotation angles varying from 1° to 45°. The PIP joint is represented by point E trajectory, while the DIP joint is represented by point F trajectory.

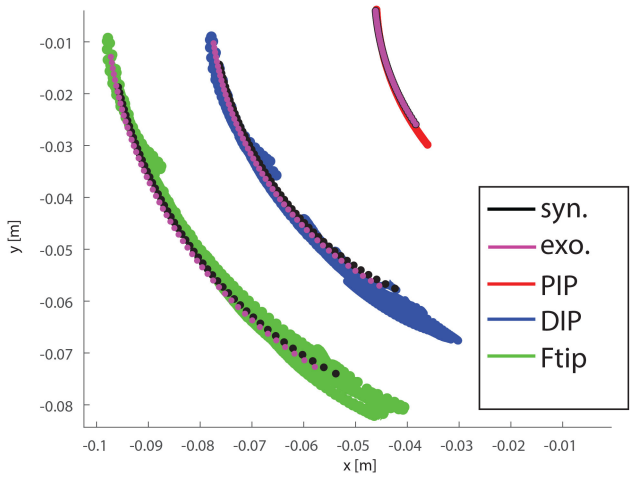

Fig. 10. Representative trajectories comparison: in red, trajectories of points E (corresponding to the PIP joint position), in blue F (corresponding to the DIP joint position), and in green Q (corresponding to the fingertip position) for different values of MCP angle. Trajectories are acquired using the optical tracking system. Black dots represent the theoretical exoskeleton trajectory, while magenta dots correspond to the first postural synergy [43].

IV. Device Control

A. Tracking

A key aspect of controlling the device is represented by tracking the hand and wrist motions. The adopted solution relies on multiple inertial measurement units (IMUs), low-cost electronic devices embedding an accelerometer, and a gyroscope on a single board. This solution is the optimal tradeoff between the accuracy of the estimation, wearability, and lightness. More in detail, we developed data acquisition and processing software capable of translating online IMU measurements into biomechanical information (i.e., the orientation of the hand with respect to the forearm). The resulting algorithm is able to: 1) record the user's motion (e.g., wrist exercises suggested and guided by the physiotherapist); 2) monitor/control exercises played back by the exoskeleton; and 3) analyze the patient's wrist articulation range of motion and consequential improvements.

To this end, we exploited two Xsens Mi-3 (Xsens, NL) embedding an accelerometer, a gyroscope, and a magnetometer in a single chip. For the purpose of this work, we decided not to use readings provided by the magnetometer since the magnetic flux in the surrounding of the exoskeleton is not reliable. The orientation of the hand with respect to the forearm (i.e., the wrist angles) is computed by means of two sensors board. An IMU is placed on the back of the hand exoskeleton structure, whereas a second one is firmly attached to the forearm exoskeleton support (as visible in Fig. 1).

To estimate the orientation of each board, we adapted the algorithm presented in [45]. Raw data from the sensors are collected and processed by the worn microcontroller in charge of all the mathematical computations. The update rate for the system is 1 kHz.

In what follows, we briefly summarize the procedure required to calibrate the sensors and we outline the tracking algorithm. Each IMU board requires an initial calibration, which consists of two steps. In the former, the user is asked to maintain the hand stable for a second, e.g., displace the hand on a flat surface. In this phase, each IMU board collects 500 samples to estimate the gyroscope bias. In the second step, we compute the offset quaternion between the hand and the forearm.

In this article, we use quaternions to estimate the orientation of a single IMU sensor. Using quaternion allows us to overcome the problems introduced by the Euler angles, for instance, the gimbal lock problem and the issues related to the trigonometric functions.

Let ${}^{S}q_H(t)$ and ${}^{S}q_F(t)$ be the quaternions that express the orientation, with respect to the sensor reference frame Σ_S, of the frames associated with the hand and the forearm, respectively. Let ${}^{F}\hat{q}_H$ be the offset quaternions between the hand and the forearm, estimated during the aforementioned calibration phase. At a certain time instant t, the orientation of the hand referred to the forearm can be computed as

$$ {}^{F}q_H(t) = {}^{F}q_S(t) \otimes {}^{S}q_H(t) $$

where ${}^{F}q_S(t)$ is the conjugate quaternion of ${}^{S}q_F(t)$. As a final step, the resulting quaternions are converted into *Euler Angles*.

B. Actuators' Control

The complete control scheme for the wrist and hand modules is depicted in Fig. 11.

The user can select different options listed in the software GUI. The data from the user interface are sent to the device via Bluetooth. Two Bluetooth modules RN42 are used for the communication between the PC and the device. A Teensy microcontroller controls the movement of the motors and the autonomous closure mechanism. It can also receive the data related to wrist exercises; in this case, it generates a set of commands for the Open CM 9.04 control board to actuate the three XL-320 motors.

Regarding the control of the hand actuation system, since finger motion is constrained by the exoskeleton mechanical

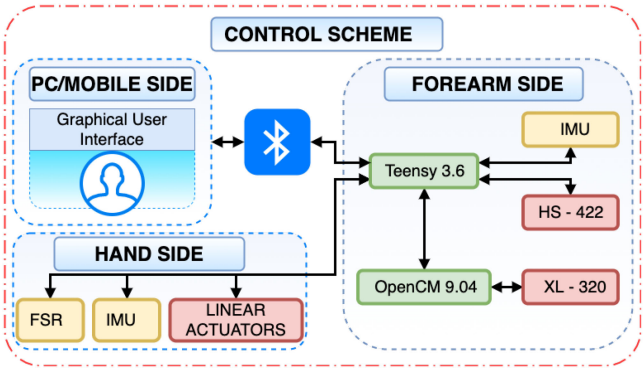

Fig. 11. Control scheme for wrist and hand exoskeleton modules.

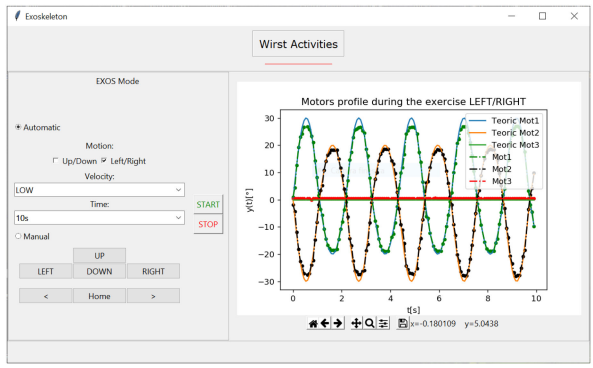

Fig. 12. GUI display during an automatic exercise layout for wrist abduction/adduction.

structure, hand configuration is directly related to actuator displacements by means of standard forward kinematics relationships. It is worth to observe that for this type of mechanism, the forward kinematic procedure depends on the user's specific biometric dimensions (e.g., the lengths of phalanges) and on displacements of finger modules. A calibration procedure included in the GUI solves this issue. Both the hand and the wrist actuators are position controlled. The proportional gain can be selected in a predefined range to regulate the stiffness of the device. The input for the control scheme is the desired movement $\boldsymbol{\theta}_{\text{des}}$ that can be assigned by the user through the GUI or previously recorded by the tracking system. $\boldsymbol{\theta}_{\text{des}}$ is a 7×1 vector, i.e., two rotation angles for the wrist and one rotation for each of the fingers. $\boldsymbol{\theta}_{\text{des}}$ values can be recorded, for example, during the execution of an exercise in which the exoskeleton is not actuated, and the hand and wrist motions are manually guided by the physiotherapist or can be loaded from an exercise database by means of a user interface. Through the inverse kinematic analysis, desired configurations are transformed into references for the actuator control systems $\boldsymbol{q}_{\text{des}}$. $\boldsymbol{q}_{\text{des}}$ is a 8×1 vector (three motor rotation angles for the wrist module and five LA strokes for the hand). Actual hand and wrist movements $\boldsymbol{\theta}$ are monitored by the tracking system and by the LA encoders during exercise execution displayed on the GUI and logged. In this first version of the device, a position-based control is proposed instead of impedance or admittance control, which is more widely used in the robotic rehabilitation area. The position control has been chosen because it is simpler to be managed by the user through the GUI.

C. Graphical User Interface

Together with the hardware design and prototyping, a GUI has been developed for managing the exoskeleton and fully exploiting its features. The main objective of the GUI is to provide the user with a simple and easy way for controlling the device, and for this reason, it was developed on the basis of the target user's requirements and feedback. The interface is divided into different sections (pages): an initial one presenting the overall system and a set of more specific ones dedicated to each function of the exoskeleton. On all the pages, a series of navigation buttons allow to easily switch between them. Each page contains the tools to control the different functions of the exoskeleton. A set of *default* parameters, chosen on the basis of the user's feedback, has been defined for each function of the exoskeleton. If the parameters are not properly defined, the exoskeleton does not perform any action. For example, if the user wants to activate an exercise with the wrist exoskeleton in automatic mode, this is not performed until all parameters such as speed, duration, and mode are properly set. Furthermore, the GUI allows to store and replay of hand and wrist motions for training and rehabilitation purposes in real time. Stored data can further be exploited for monitoring the effectiveness of the rehabilitation treatment. A cross-platform Python-based application connects the exoskeleton system via Bluetooth and displays the user the options to record/replay wrist and fingers motions. A screenshot of the GUI is reported in Fig. 12.

Three main pages help the user in selecting the desired feature.

Activities for Hand: The aim of this page is to control the hand exoskeleton. Two modes are available: *Learning Mode* and *Reproduce Mode*. *Learning Mode* is further divided into *Motion Mode* and *Grasp Mode*. The former allows to control and move one finger at a time (selectable via five checkboxes). The *Grasp* option lets the user to control all the fingers by moving only the index finger and exploiting the first postural synergy. Both modalities can be recorded and played back on demand in the *Reproduce Mode*.

Activities for Wrist: Here, the user is allowed to select two modes of use: *automatic* or *manual*. The *manual* modality enables four buttons for controlling the motion of the wrist: DOWN for flexion, UP for extension, LEFT for ulnar adduction, and RIGHT for radial abduction. Conversely, the *automatic* mode allows the user to perform some typical exercises for the wrist, such as abduction/adduction and flexion/extension movements. Paradigmatic exercises are already available in the interface. For each exercise, the user can select a running time and three different speeds (high, medium, and low). Moreover, the GUI also allows to set manually a specific time span and a certain speed value for the exercise.

Learning Mode for Wrist: The aim of this page is to let the exoskeleton learn exercises, performed, for example, by a

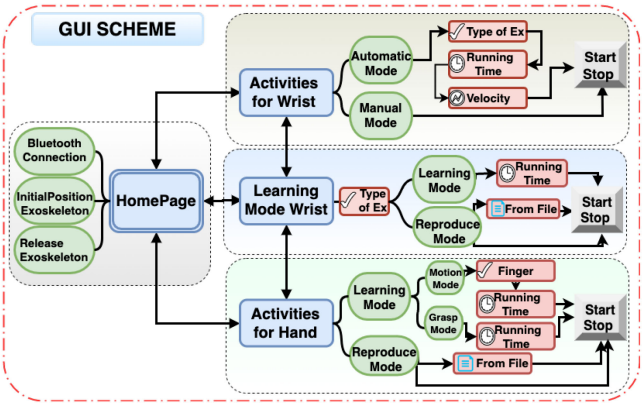

Fig. 13. GUI flowchart for wrist and hand exercises. Light blue blocks represent GUI pages, green blocks are the operations inside the page, and light red blocks show editable and selectable options.

physiotherapist, and then play back them. During the *Learning* phase, wrist exoskeleton motors are disabled. In this way, the physiotherapist can freely move the wrist while the exoskeleton tracking system records these movements. Regarding wrist exercises, IMU data are acquired and elaborated with a frequency of 200 Hz and saved in a file by GUI software. In *Reproduce* mode, a profile previously recorded and saved is loaded from the archive and played back. The Learning/Reproduce modes are also available for the hand module, and also in this case, in the *Learning* mode, the system acquires samples at 200 Hz. In fingers Learning mode, the LAs are moved using the FSR-based control detailed in Section III-B.

It is worth observing that the wrist and hand modules have been managed in two different ways, and in particular, in the *Activities for Hand* module, the Automatic Mode is not present. Since hand structure is more complex than the wrist and the actuation is realized in a completely different way, in accordance with the user involved in the design and his physiotherapist, the possibility of executing exercises with a prerecorded profile has been deemed not necessary. The GUI homepage includes some general functions: it is used to connect/disconnect to the exoskeleton's Bluetooth to access all the pages and to control the closure mechanism. In particular, the closure mechanism is activated/deactivated through two dedicated buttons. Furthermore, through this page, the user or the physiotherapist can reset the initial position of the exoskeleton and set/deactivate the initial position of all actuators, including the motors used to control the closure mechanism. A flowchart reporting all the GUI components is reported in Fig. 13.[3]

Both hardware and software development consider the patient's safety in case of exoskeleton malfunctioning or in case of physical problems of the person. Concerning the developed device, the exoskeleton can be deactivated at any time by pressing a button on the Teensy board that disables all the motors by removing the torque from all of them. The same command can be set via software through the "Stop" button present on all the GUI pages. The motor that is used to control the closing mechanism is disabled as soon as the mechanism is opened. In case of motor failure, torque is immediately disabled, allowing the machine to be opened manually.

[3]A demonstrative video is available as multimedia attachment of this article and also at the following link: [Online]. Available: http://sirslab.dii.unisi.it/exoskeleton/video2.mp4

V. Tests and Evaluation

Since the modules of the exoskeleton are designed according to user's specific characteristics and needs, in the testing and evaluation phase, a single patient was involved, according to the "single-case-design" methodology, a procedure that is often employed in the clinical field in which an individual is the only unit of data analysis which is capable of providing rigorous experimental evidence [46].

The tests are aimed at verifying the performance of the device in terms of accuracy in the execution of specific exercises. Different typologies of exercises suggested by the physiotherapist, involving both the hand and the wrist, were considered.

The subject gave his written informed consent to participate and was able to discontinue participation at any time during the experiments. The experimental evaluation protocols followed the declaration of Helsinki, and there was no risk of harmful effects on subject's health. Data were recorded in conformity with the European General Data Protection Regulation 2016/679, stored locally, and used only for the postprocessing evaluation procedure. Note that no sensible data were recorded.

A stepwise validation was conducted. In the former step, we focused on wrist tracking and actuation, whereas in the second, fingers were considered. Finally, the wrist and hand were evaluated together. The system was evaluated on a subject with severe limitations in extension motion (movement in flexion are with reduced problems), some limitations in radial adduction and ulnar abduction, and severe limitations in opening/closing the hand.

A. Wrist Evaluation

To evaluate the proposed exoskeleton in wrist-based exercise performance, we conducted three different experiments. In all the experiments, precision in following a desired profile was considered as a metric and measured by means of the root mean square error (RMSE). Similarly to [47], for each trial, we define this quantity as $\text{RMSE}_t = \sqrt{\frac{1}{N}\sum_{i=1}^{N}(y_{t,i} - y_i)^2}$, where N is the number of samples in a trial, y_i is the actual value, and $y_{t,i}$ is the corresponding target value. The mean among the RMSE values was used to analyze the tracking performance throughout the whole experiment. It is worth noticing that the tracking RMSE is a suitable metric to evaluate the rapidity and the accuracy of the robot motions. This is due to the fact that RMSE increases both if the exoskeleton is slow in updating the control variable and if it does not reach the target value.

1) Wrist Test 1—Flexion/Extension: The first set of tests was carried out to evaluate the system accuracy in following a specific desired motion. A predefined set of movements was generated with the aim of covering the entire patient's wrist range of

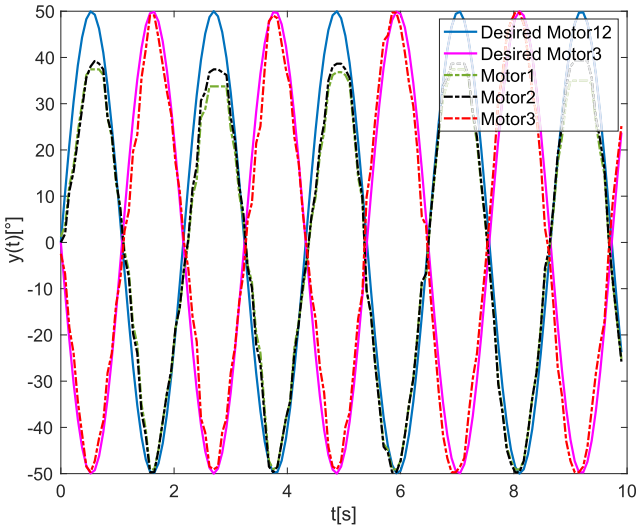

Fig. 14. Wrist test 1: automatic wrist flexion and extension. Reference and actual motor rotations during one of the trials.

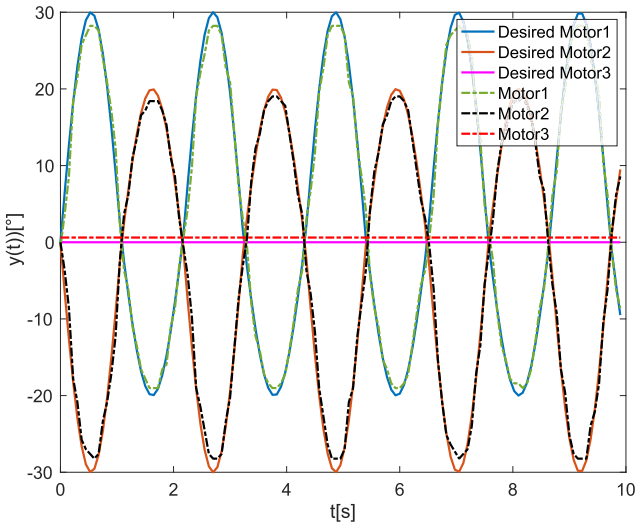

Fig. 15. Wrist test 2: ulnar adduction and radial abduction. Reference and actual motor rotations during one of the trials.

motion. Three different motion speeds were considered. As introduced in Section III, wrist flexion/extension is obtained by setting the same profile to actuators *Motor1* and *Motor2* and the opposite to actuator *Motor3*. To simulate a realistic flexion/extension exercise performed by a physiotherapist, the following reference values were set to the actuators:

$$\varphi_{1,\text{des}} = \varphi_{2,\text{des}} = \alpha \sin(\omega t),\ \varphi_{3,\text{des}} = -\alpha \sin(\omega t)$$

with $\alpha = 50°, \omega = 3.0, 4.0$ or $5.0\,\text{rads}^{-1}$, and $0 < t < 10\,\text{s}$. The three values of ω represent "low," "moderate," and "high" speed of wrist flexion/extension, respectively. The internal encoder of the motors was used to record the actual angular value. A total of 20 trials for each speed were repeated, and each one lasted 10 s. Desired and measured values of rotation angles of a representative trial are reported in Fig. 14; the figure shows how the actuators are able to follow the profile for the entire duration of the exercise.

Results: We observed that the average RMSEs in following the reference among the 60 trials were $5.39° \pm 0.25°$, $5.25° \pm 0.24°$, and $5.55° \pm 0.25°$ for *Motor1*, *Motor2*, and *Motor3*, respectively. Moreover, a statistical analysis was conducted for supporting the outcome of the experiment and for investigating the potential dependencies of errors on the exercise speed. Data were not normally distributed; thus, for each motor, a Kruskal–Wallis H test was conducted to determine if there were differences in RMSEs between actuating the exoskeleton with different values of ω: "low" ($\omega = 3.0\,\text{rads}^{-1}$), "moderate" ($\omega = 4.0\,\text{rads}^{-1}$), and "high" ($\omega = 5.0\ \text{rads}^{-1}$) speeds. Distributions of RMSEs were similar for all the groups, as assessed by the visual inspection of a boxplot.

For what concern *Motor1*, median RMSEs were statistically significantly different between groups, $\chi^2(2) = 47.79, p < 0.001$. Subsequently, pairwise comparisons were performed using Dunn's (1964) procedure with a Bonferroni correction for multiple comparisons. This post hoc analysis revealed statistically significant differences in median RMSE values between the "low" (3.69) and "moderate" (4.97) ($p = 0.004$) speeds, "low" and "high" (6.32) ($p < 0.001$), and "moderate" and "high" ($p = 0.001$) speeds. Such a test was also exploited in the next comparisons. For the sake of readability in what follows, we refer only as "pairwise comparison." Similar results were obtained for *Motor2*. Medians of RMSEs were statistically significantly different between different values of ω, $\chi^2(2) = 46.81, p < 0.001$. The subsequent pairwise comparison analysis revealed statistically significant differences in median RMSE values between the "low" (3.67) and "moderate" (4.68) ($p = 0.005$) speeds, "low" and "high" (6.11) ($p < 0.001$), and "moderate" and "high" ($p = 0.001$) speeds. As expected, *Motor3* also follows the same behavior as *Motor1* and *Motor2*. RMSE medians were statistically significantly different considering the three speeds, $\chi^2(2) = 48.04$, $p < 0.001$. Also, in this case, pairwise comparisons were performed. The post hoc test revealed statistically significant differences in median RMSE values between the "low" (3.86) and "moderate" (5.14) ($p = 0.004$) speeds, low and "high" (6.48) ($p < 0.001$), and "moderate" and "high" ($p = 0.001$) speeds.

2) Wrist Test 2—Adduction/Abduction: Then, we simulated the ulnar adduction and radial abduction. To reproduce this behavior, *Motor3* was maintained steady, whereas motors *Motor1* and *Motor2* pulled their tendons in opposite directions, as explained in Section III. Desired and measured values of rotation angles of a representative trial are reported in Fig. 15. As in the previous experiment, with the aim at evaluating the exoskeleton in the whole range of motion of the wrist, the following reference profiles were used as motors control input:

$$\varphi = \alpha \sin(\omega t),\ \alpha = \begin{cases} 30° \text{ if } \sin(\omega t) > 0 \\ 20° \text{ if } \sin(\omega t) < 0 \end{cases}$$

$$\varphi_{1,\text{des}} = \varphi,\ \varphi_{2,des} = -\varphi,\ \varphi_{3,des} = 0$$

$\omega = 3.0, 4.0,$ or $5.0\ \text{rads}^{-1}$ and $0 < t < 10$ s. A total of 20 consecutive trials were repeated for each value of ω, for a total

of 60 repetitions. Desired rotation angle and real motor value were recorded and analyzed.

Results: We observed that the average RMSEs among all the trials in tracking the requested profile were $4.06^\circ \pm 0.14^\circ$, $3.64^\circ \pm 0.15^\circ$, and $0.17^\circ \pm 0.12^\circ$ for *Motor1*, *Motor2*, and *Motor3*, respectively.

The same statistical analysis conducted in the previous experiment was also repeated to analyze the results concerning adduction/abduction movements. Data of *Motor3* were excluded from the analysis since the motor was maintained stable and the recorded errors were due only to measurement noise. The mean among all the trials is 0.17° with a standard deviation less than 0.12°; this means that the motor remained stable for all the trials, and the recorded error is due to the mechanical resolution of the encoder. Data of *Motor1* and *Motor2* were not normally distributed, thus a Kruskal–Wallis H test was conducted to determine if there were differences in RMSEs between moving the motor with different values of ω, i.e., "low" ($\omega = 3.0$ rads^{-1}), "moderate" ($\omega = 4.0$ rads^{-1}), and "high" ($\omega = 5.0$ rads^{-1}) speeds. Distributions of RMSEs were similar for all the groups, as assessed by visual inspection of a boxplot.

Regarding *Motor1*, median RMSEs were statistically significantly different between groups, $\chi^2(2) = 49.72, p < 0.001$. Multiple pairwise comparisons were performed and revealed statistically significant differences in median RMSE values between the low (3.00) and moderate (4.03) ($p < 0.001$) speeds, low and high (5.04) ($p < 0.001$), and moderate and high ($p = 0.003$) speeds. Comparable results were obtained analyzing the results of *Motor2*. Medians of RMSEs were statistically significantly different between the three values of ω, $\chi^2(2) = 50.37$, and $p < 0.001$. Following pairwise comparisons revealed statistically significant differences in median RMSE values between the low (2.43) and moderate (3.63) ($p = 0.001$) speeds, low and high (4.73) ($p = 0.002$), and moderate and high ($p < 0.001$) speeds.

3) Wrist Test 3—Record/Playback: An additional test was conducted for verifying the capability of recording an exercise performed by a physiotherapist and reproducing it with the exoskeleton. A physiotherapist and the above-introduced patient with severely limited wrist mobility were involved in this test. We asked the physiotherapist to gently move the hand of the patient for 10 s while the system was recording the hand orientation with respect to the forearm (i.e., the wrist angles). Ten adduction/abduction and ten flexion/extension exercises were carried out. A representative trial for this type of trial is reported in Fig. 16. The figure shows that the system is able to record hand motion with respect to the forearm through the tracking system and playback motions through the exoskeleton. Ten consecutive trials were performed by using the same profile recorded by the physiotherapist. For each repetition, the real values of the motors' rotation angles were recorded. **Results:** The average RMSEs in tracking the trajectory previously recorded by the physiotherapist were $3.15^\circ \pm 0.54^\circ$ for *Motor1*, $3.51^\circ \pm 0.62^\circ$ for *Motor2*, and $2.59^\circ \pm 0.76^\circ$ for *Motor3*.

In Table II, all the results described above are reported in terms of average RMSEs.

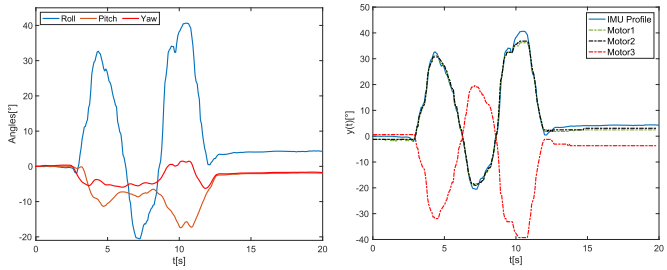

(a) (b)

Fig. 16. Wrist test 3: record/playback. (a) Roll, pitch, yaw angles measured by the tracking system. (b) Learning mode: Flexion and extension angles as recorded by the physiotherapist and corresponding motor rotations.

TABLE II
SYNTHESIS OF THE WRIST EVALUATION RESULTS IN TERMS OF AVERAGE RMSES

Test	Nr. Trials	Motor1 Average RMSEs [deg.]	Motor2 Average RMSEs [deg.]	Motor3 Average RMSEs [deg.]
Wrist test 1	60	5.39 ± 0.25	5.25 ± 0.24	5.55 ± 0.25
Wrist test 2	60	4.06 ± 0.14	3.64 ± 0.15	0.17 ± 0.12
Wrist test 3	20	3.15 ± 0.54	3.51 ± 0.62	2.59 ± 0.76

B. Hand Evaluation

In the second stage, the performance of the hand part of the exoskeleton has been considered.

1) Hand Test 1—Single Finger: We started the evaluation of the hand module considering the capability of the exoskeleton in the following therapeutic exercises using four fingers. The first experiment consisted of an exercise of individual fingers carried out by the physiotherapist. In this exercise, the physiotherapist moved a finger (i.e., index, middle, ring, little finger) by either pulling the finger down or pushing the finger up. The FSR sensors installed under the base of the finger (see Figs. 6 and 7) recognized this movement and the LA moved accordingly. Two threshold values were defined in order to recognize the real finger's movement and avoid problems related to misalignment or nonproper positioning of the finger module on the hand. Threshold values were defined as a tradeoff between readiness and reliability in identifying finger motion. A too wide threshold window (i.e., the distance between the upper and lower thresholds) would require the physiotherapist to apply relatively high forces for moving the exoskeleton and the resulting finger motion could result forced. On the other hand, a too tight threshold window could be too sensitive with respect to noise and sensor errors. Since the optimal threshold values depend on several factors (sensor features, assembly accuracy, but also

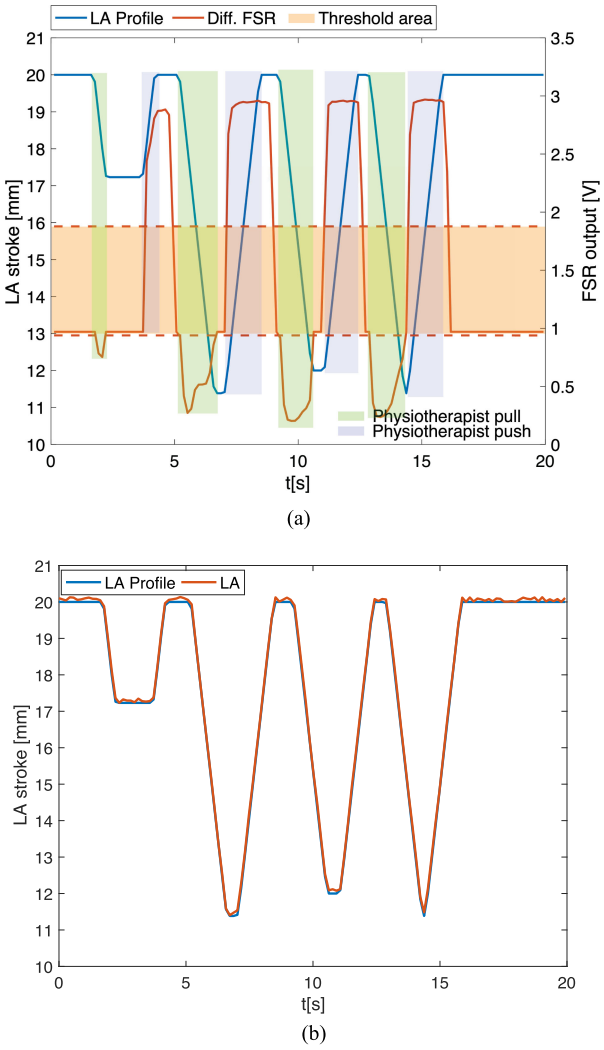

Fig. 17. Hand test 1: single-finger exercise guided by a physiotherapist. (a) Recording phase: the differential FSR sensors measure (red line), threshold values for generating LA reference (orange area), and corresponding LA reference (blue line). (b) Reference (blue line) and real actuator displacement (red line).

user's specific characteristics), their values can be assessed and modified by means of a suitable calibration procedure included in the GUI that can be run at the beginning of the exercise or any time it is needed. In particular, in the experiments described in this article, carried out by a single user in the same exercise session, the lower threshold (expressed in terms of FSR output voltage) was set to 1 V, and the upper one was set to 1.9 V. Finger movement was recorded, and when the physiotherapist finished the exercise, all the data related to the exercise were saved and available for future analyses of for repeating the exercise. Fig. 17(a) shows the data acquired in the recording phase; the orange curve represents the FSR reading when the physiotherapist pushes and pulls the fingertip, while the blue curve represents the position of the actuator. The trial started with the finger in a starting position, in which the finger is almost straight but relaxed, and therefore, both FSRs recorded a force within the threshold limits. As soon as the physiotherapist pressed the fingertip upward, the FSR under the back end of the finger base measured a force that triggers the movement of the LA to move in the backward direction resulting in the finger moving up, as depicted by the plot with the first blue slope down. Similarly, when the physiotherapist pressed the fingertip downward, the FSR installed under the front end of the finger base detected the force and the LA started to move forward, which resulted in the finger moving downward, as can be seen by the upward slope of the blue line in the plot. The physiotherapist could stop pressing up or down at any stage to generate a variety of motions. Fig. 17(b) shows the profile recorded by the physiotherapist in moving the finger up and down by pushing down or pulling up the fingertip. The blue curve represents the recorded data, while the red plot represents the trajectory followed by the LA. It can be seen that the LA followed the recorded trajectory.

Results: To evaluate the accuracy and fidelity in reproducing the physiotherapist's motion, we compared the desired position of the LA (memorized during the recording phase) with the one obtained in the following play-back phase. In these quantitative evaluations, three LAs over the five employed in the exoskeleton were activated and analyzed for the sake of conciseness since their behaviors were similar. A total of 40 trials of recording and playback were acquired for each motor. The resulting average RMSE was 0.34 ± 0.07 mm for LA1. Similarly, for LA2 and LA3, the RMSE was 0.50 ± 0.04 mm and 0.38 ± 0.05 mm, respectively.

2) Hand Test 2—Synergy-Based Hand Motion: In this experiment, the physiotherapist moved the finger just like in the case of a single-finger motion, but here the difference is in the actuation; instead of moving a single finger, this time the whole hand (all fingers and thumb) moved in accordance with the first postural synergy. The data were saved and reused later for standalone exercises. Fig. 18(a) shows the plot for this exercise. As it can be seen, as soon as the physiotherapist pushed down or pulled up the finger, the FSRs detected the corresponding force applied on the fingertip, and consequently, all the LAs moved forward or backward to move the finger down or up, respectively. The orange line in the plot [see Fig. 18(a)] shows the FSR data, whereas the other five lines depict the movement of the fingers. Similarly, Fig. 18(b) shows the stroke profile followed by the LAs as recorded by the physiotherapist.

Results: Following the approach of Hand test 1, 40 trials were recorded and analyzed in this experiment also. RMSE in following the desired position was 0.42 ± 0.12 mm, 0.54 ± 0.13 mm, and 0.53 ± 0.11 mm for LA1, LA2, and LA3, respectively.

3) Hand Test 3—Grasping Task: This experiment replicated a real scenario in which a physiotherapist helped the patient in grasping an object, such as a bottle. The physiotherapist started moving a single finger by following the above-mentioned approach and stopped it at the desired position. In this experiment, the physiotherapist was able either to move all the fingers individually to establish a grasp or to exploit the first synergy (i.e., moving a single finger for controlling the whole hand). Also, in this case, at the end of the exercise, all the data were recorded to be reproduced in future therapy sessions. Fig. 19(a) shows the FSR measures when the physiotherapist formed a stable grasp and blue line shows the resulting LA position.

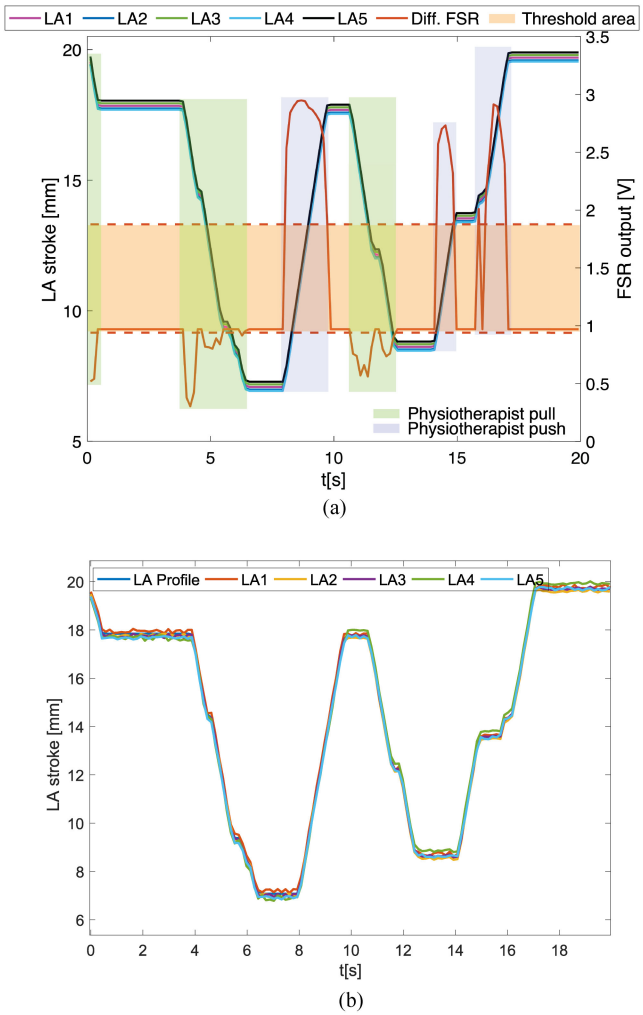

Fig. 18. Hand test 2: synergy-based actuation of all the fingers, guided by a physiotherapist. (a) Differential FSR sensors measure (red line), threshold values for generating LA reference (orange area), and corresponding LA reference for all the fingers. (b) Reference (blue) and real actuator displacements for all the fingers.

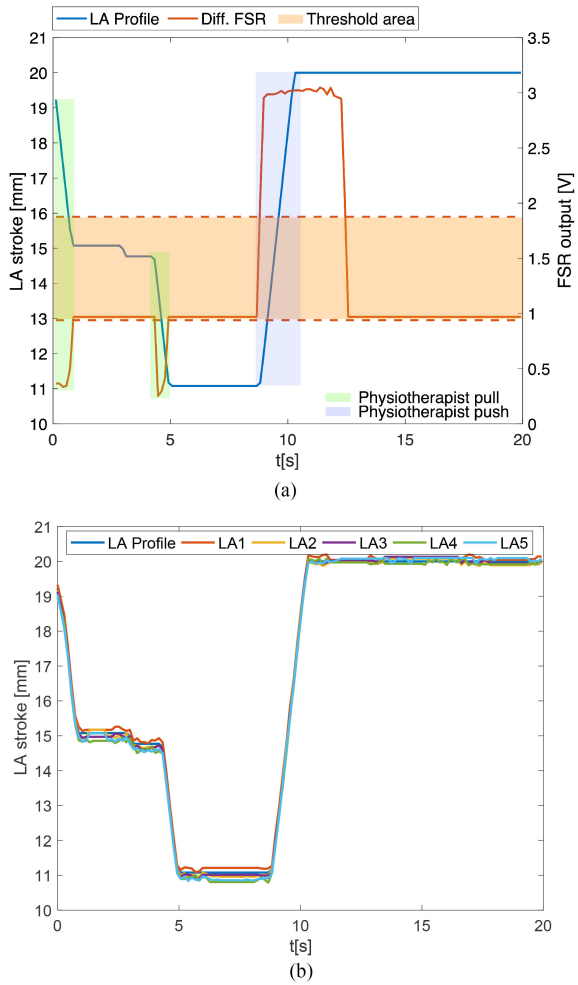

Fig. 19. Hand test 3: grasp exercise performed by a physiotherapist. (a) Recording phase: the differential FSR sensors measure (red line), threshold values for generating LA reference (orange area), and corresponding LA reference (blue line). (b) Grasp exercise reproduced without physiotherapist: reference (blue line) and real displacements of the LAs.

Similarly, Fig. 19(b) reports the comparison between the desired trajectory and the one followed by all the LAs to playback the physiotherapist movement. Finally, Fig. 20 shows the action of grasping a bottle with the exoskeleton using the physiotherapist recordings. It is worth noticing that the patient without the exoskeleton would not have been able to grasp the object due to the hand muscles limitations.

Results: Analysis of the RMSE of the motors was also conducted at the end of *Hand Test 3* experiment. LA1 reported an RMSE of 0.31 ± 0.03 mm, LA2 0.36 ± 0.03 mm, and LA3 0.35 ± 0.02 mm.

In conclusion, for all the conducted hand tests, the RMSE of the motors is comparable with the error given by the resolution of the feedback potentiometer and the mechanical properties of the hardware (see Table I). These results, given in Table III, support the hardware choice and the mechanical design of the exoskeleton that is able to reproduce the desired motion with high precision and accuracy.

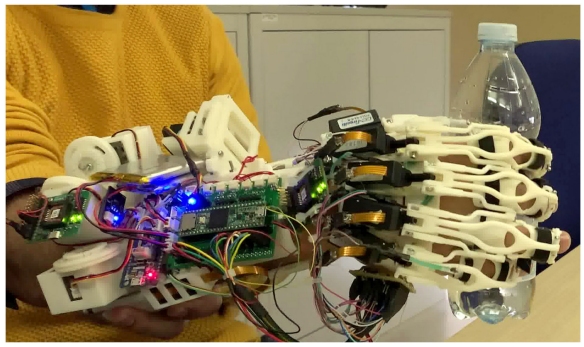

Fig. 20. Grasp exercise autonomously reproduced by the patient without physiotherapist.

It is worth to notice that the errors measured in the LAs are very limited; however, such errors refer to actuators only and do not take into account the overall deformation of the transmission system. An evaluation of the actual hand module displacement errors and their relationship with the mechanical transmission

TABLE III
SYNTHESIS OF THE HAND EVALUATION RESULTS IN TERMS OF AVERAGE RMSES

Test	Nr. Trials	LA1 Average RMS Es [mm]	LA2 Average RMS Es [mm]	LA3 Average RMS Es [mm]
Hand test 1	40	0.34 ± 0.07	0.50 ± 0.04	0.38 ± 0.05
Hand test 2	40	0.42 ± 0.12	0.54 ± 0.13	0.53 ± 0.11
Hand test 3	40	0.31 ± 0.03	0.36 ± 0.03	0.35 ± 0.02

structural properties would require extensive analysis and experimental activity; the results would depend on user's specific characteristics (e.g., residual muscle capabilities or presence of spasticity) and will be the focus of future investigations on this topic.

C. Summary of User's Evaluation

The exoskeleton is quite comfortable and does not strain excessively the user due to its limited mass (around 500 g), the distribution of inertia, and the use of soft materials in some parts, for instance, the rings connecting the finger module components to the phalanges that are made in TPU. The overall system can work for about 3 h with batteries; this duration was evaluated as suitable for a training session by the user, and in case the rehabilitation process needs more time, it can be connected by a USB cable to a power source. With respect to the preliminary version presented in [39] and notwithstanding the introduced hand actuation system, the new version of the exoskeleton presents a significantly improved wearability, thanks to the automatic closure system. To preliminary justify what we have just started, we asked for further feedback from a potential user, with reduced mobility, on the time he takes to fix the exoskeleton compared to [39]. In a preliminary qualitative evaluation, it was found that the time he takes to wear and fix the exoskeleton is less than half of the one required by the preliminary version. This simplification is mainly due to the automatic closure system. The device can autonomously be worn by a user with no or little mobility reduction. If the user has limited arm mobility, an external support is still needed in the wearing process; however, it is significantly simplified and shortened.

The user positively evaluated the training process and reported that after a training session, his hand and wrist moved more freely, so the device represents an effective means for his rehabilitation process. He also appreciated the GUI that allowed him to easily control the exercises and that, thanks to the batteries and to the Bluetooth connection, the system is wireless. The availability of a set of prerecorded simple exercises is another useful feature. It allows to use the device without any external support. He furthermore positively evaluated the possibility of following the GUI exercise by means of diagrams.

The user also indicated some points that still need to be improved. In particular, notwithstanding the automatic closure system is a useful support; the possibility of wearing the whole device autonomously is still difficult in case of reduced mobility. The overall encumbrance should further be limited by optimizing the size of mechanic and electronic components. Finally, he would appreciate the simplification in the assemble/disassemble procedure of the modules so that it can be managed with only one hand.

VI. CONCLUSION

In this article, we presented the main features in terms of design and control of a hand/wrist exoskeleton for rehabilitation and training. The device has been developed to enhance patient independence and autonomy in the rehabilitation and training phase, reducing the time and the efforts needed by a physiotherapist or an external trainer.

This main objective was pursued by developing a modular device that can be easily worn. This design criterion guided the realization of the locking mechanism that automatically fastens the wrist support to the patient's forearm and the wireless connection to the PC. Another way to increase patient's autonomy is represented by the possibility of recording exercises guided by the physiotherapist by means of device sensors and replay them any time in other sessions. The system has been developed following a modular approach so that the user can personalize it according to her/his needs. In this article, the integrated wrist/hand system is presented; however, wrist and hand modules can be used jointly or independently on the basis of user's needs. The hand module can further be divided at a finger level, and single fingers can be actuated. Also the GUI has been developed to manage single or multiple modules.

The proposed device represents a useful tool in the telerehabilitation context, whose importance has became very relevant over the past few months. The possibility of loading personalized exercises and to record and replay an activity guided by the physiotherapist allows reducing the need of the face-to-face interaction between the patient and the physiotherapist.

Moreover, we showed some rehabilitation exercises for the wrist, for the single finger, and for the whole hand, in which exoskeleton motion was defined by means of specific mathematical functions or recorded by a demonstration realized by a physiotherapist and then autonomously reproduced.

It is worth to underline that in this work, end-users, i.e., patients suffering of upper-limb disabilities and motion limitations, have been continuously involved throughout the different phases of the project, i.e., from the very preliminary design steps to the prototype development and testing.

The exoskeleton presented in this article has a technology readiness level 4 and its overall hardware structure is going to be further optimized in the next future. In a successive phase of the work, the device development will further proceed taking into account users' and physiotherapists' specific comments and suggestions, specifically the design of finger modules will

further be developed to reduce their size, and an ad hoc App for the most common smartphones or tablets will be developed and released to improve the accessibility for the users. Finally, the hardware structure will further be enhanced, the objective is to allow a patient with limited arm and hand motion capabilities to assemble and disassemble the different modules and to wear it autonomously.

REFERENCES

[1] World Health Organization, *World Health Statistics 2016: Monitoring Health for the SDGs Sustainable Development Goals*. Geneva, Switzerland: World Health Org., 2016.

[2] E. M. Agree, "The potential for technology to enhance independence for those aging with a disability," *Disabil. Health J.*, vol. 7, no. 1, pp. S33–S39, 2014.

[3] M. A. Lim and R. Pranata, "Letter to the editor regarding 'the challenging battle of mankind against COVID-19 outbreak: Is this global international biological catastrophe the beginning of a new era?—Is telehealth the future of orthopaedic and rehabilitation in post-COVID-19 era?" *J. Orthopaedic Surg.*, vol. 28, no. 3, pp. 1–3, 2020.

[4] P. S. Lum, S. B. Godfrey, E. B. Brokaw, R. J. Holley, and D. Nichols, "Robotic approaches for rehabilitation of hand function after stroke," *Amer. J. Phys. Med. Rehabil.*, vol. 91, no. 11, pp. S242–S254, 2012.

[5] C. Bütefisch, H. Hummelsheim, P. Denzler, and K.-H. Mauritz, "Repetitive training of isolated movements improves the outcome of motor rehabilitation of the centrally paretic hand," *J. Neurological Sci.*, vol. 130, no. 1, pp. 59–68, 1995.

[6] H. Krebs, N. Hogan, B. Volpe, M. Aisen, L. Edelstein, and C. Diels, "Overview of clinical trials with mit-manus: A robot-aided neuro-rehabilitation facility," *Technol. Health Care*, vol. 7, no. 6, pp. 419–423, 1999.

[7] Z. Yue, X. Zhang, and J. Wang, "Hand rehabilitation robotics on poststroke motor recovery," *Behav. Neurol.*, vol. 2017, 2017, Art. no. 3908135.

[8] L. Dovat *et al.*, "HandCARE: A cable-actuated rehabilitation system to train hand function after stroke," *IEEE Trans. Neural Syst. Rehabil. Eng.*, vol. 16, no. 6, pp. 582–591, Dec. 2008.

[9] M. Bouzit, G. Burdea, G. Popescu, and R. Boian, "The Rutgers master II-new design force-feedback glove," *IEEE/ASME Trans. Mechatronics*, vol. 7, no. 2, pp. 256–263, Jun. 2002.

[10] O. Lambercy, L. Dovat, R. Gassert, E. Burdet, C. L. Teo, and T. Milner, "A haptic knob for rehabilitation of hand function," *IEEE Trans. Neural Syst. Rehabil. Eng.*, vol. 15, no. 3, pp. 356–366, Sep. 2007.

[11] L. Masia, H. I. Krebs, P. Cappa, and N. Hogan, "Design and characterization of hand module for whole-arm rehabilitation following stroke," *IEEE/ASME Trans. Mechatronics*, vol. 12, no. 4, pp. 399–407, Aug. 2007.

[12] R. Conti *et al.*, "Kinematic synthesis and testing of a new portable hand exoskeleton," *Meccanica*, vol. 52, no. 11, pp. 2873–2897, 2017.

[13] N. Secciani, M. Bianchi, E. Meli, Y. Volpe, and A. Ridolfi, "A novel application of a surface electromyography-based control strategy for a hand exoskeleton system: A single-case study," *Int. J. Adv. Robot. Syst.*, vol. 16, no. 1, pp. 1–13, 2019.

[14] N. Secciani, A. Topini, A. Ridolfi, E. Meli, and B. Allotta, "A novel point-in-polygon-based sEMG classifier for hand exoskeleton systems," *IEEE Trans. Neural Syst. Rehabil. Eng.*, vol. 28, no. 12, pp. 3158–3166, Dec. 2020.

[15] F. Zhang, L. Hua, Y. Fu, H. Chen, and S. Wang, "Design and development of a hand exoskeleton for rehabilitation of hand injuries," *Mech. Mach. Theory*, vol. 73, pp. 103–116, 2014.

[16] C. J. Nycz, T. Bützer, O. Lambercy, J. Arata, G. S. Fischer, and R. Gassert, "Design and characterization of a lightweight and fully portable remote actuation system for use with a hand exoskeleton," *IEEE Robot. Automat. Lett.*, vol. 1, no. 2, pp. 976–983, Jul. 2016.

[17] H. C. Fischer, K. Stubblefield, T. Kline, X. Luo, R. V. Kenyon, and D. G. Kamper, "Hand rehabilitation following stroke: A pilot study of assisted finger extension training in a virtual environment," *Topics Stroke Rehabil.*, vol. 14, no. 1, pp. 1–12, 2007.

[18] C. D. Takahashi, L. Der-Yeghiaian, V. Le, and S. C. Cramer, "A robotic device for hand motor therapy after stroke," in *Proc. IEEE 9th Int. Conf. Rehabil. Robot.*, 2005, pp. 17–20.

[19] E. Koeneman, R. Schultz, S. Wolf, D. Herring, and J. Koeneman, "A pneumatic muscle hand therapy device," in *Proc. IEEE 26th Annu. Int. Conf. Eng. Med. Biol. Soc.*, 2004, pp. 2711–2713.

[20] I. B. Abdallah, Y. Bouteraa, and C. Rekik, "Design and development of 3D printed myoelectric robotic exoskeleton for hand rehabilitation,," *Int. J. Smart Sens. Intell. Syst.*, vol. 10, no. 2, pp. 341–366, 2017.

[21] T. Bützer, O. Lambercy, J. Arata, and R. Gassert, "Fully wearable actuated soft exoskeleton for grasping assistance in everyday activities," *Soft Robot.*, vol. 8, no. 2, pp. 128–143, 2021.

[22] U. A. Hofmann, T. Bützer, O. Lambercy, and R. Gassert, "Design and evaluation of a Bowden-cable-based remote actuation system for wearable robotics," *IEEE Robot. Automat. Lett.*, vol. 3, no. 3, pp. 2101–2108, Jul. 2018.

[23] P. Heo, G. M. Gu, S.-J. Lee, K. Rhee, and J. Kim, "Current hand exoskeleton technologies for rehabilitation and assistive engineering," *Int. J. Precis. Eng. Manuf.*, vol. 13, no. 5, pp. 807–824, 2012.

[24] T. du Plessis, K. Djouani, and C. Oosthuizen, "A review of active hand exoskeletons for rehabilitation and assistance," *Robotics*, vol. 10, no. 1, 2021, Art. no. 40.

[25] T. Shahid *et al.*, "Moving toward soft robotics: A decade review of the design of hand exoskeletons," *Biomimetics*, vol. 3, no. 3, 2018, Art. no. 17.

[26] H. I. Krebs *et al.*, "Robot-aided neurorehabilitation: A robot for wrist rehabilitation," *IEEE Trans. Neural Syst. Rehabil. Eng.*, vol. 15, no. 3, pp. 327–335, Oct. 2007.

[27] A. Gupta, M. K. O'Malley, V. Patoglu, and C. Burgar, "Design, control and performance of ricewrist: A force feedback wrist exoskeleton for rehabilitation and training," *Int. J. Robot. Res.*, vol. 27, no. 2, pp. 233–251, 2008.

[28] N. W. Bartlett *et al.*, "A soft robotic orthosis for wrist rehabilitation," *J. Med. Devices*, vol. 9, no. 3, 2015, Art. no. 030918.

[29] N. Rehmat, J. Zuo, W. Meng, Q. Liu, S. Q. Xie, and H. Liang, "Upper limb rehabilitation using robotic exoskeleton systems: A systematic review," *Int. J. Intell. Robot. Appl.*, vol. 2, no. 3, pp. 283–295, 2018.

[30] G. Turchetti, N. Vitiello, S. Romiti, E. Geisler, and S. Micera, "Why effectiveness of robot-mediated neurorehabilitation does not necessarily influence its adoption," *IEEE Rev. Biomed. Eng.*, vol. 7, pp. 143–153, 2014.

[31] A. D. V. Dabbs *et al.*, "User-centered design and interactive health technologies for patients," *Comput. Inform. Nurs.*, vol. 27, no. 3, 2009, Art. no. 175.

[32] P. Lehoux and D. Grimard, "When robots care: Public deliberations on how technology and humans may support independent living for older adults," *Social Sci. Med.*, vol. 211, pp. 330–337, 2018.

[33] C. J. Nycz, T. B. Meier, P. Carvalho, G. Meier, and G. S. Fischer, "Design criteria for hand exoskeletons: Measurement of forces needed to assist finger extension in traumatic brain injury patients," *IEEE Robot. Automat. Lett.*, vol. 3, no. 4, pp. 3285–3292, Oct. 2018.

[34] Q. A. Boser, M. R. Dawson, J. S. Schofield, G. Y. Dziwenko, and J. S. Hebert, "Defining the design requirements for an assistive powered hand exoskeleton: A pilot explorative interview study and case series," *Prosthetics Orthotics Int.*, vol. 45, no. 2, pp. 161–169, 2021.

[35] J. Lee and T. L. Kunii, "Model-based analysis of hand posture," *IEEE Comput. Graph. Appl.*, vol. 15, no. 5, pp. 77–86, Sep. 1995.

[36] H. In, B. B. Kang, M. Sin, and K.-J. Cho, "Exo-Glove: A wearable robot for the hand with a soft tendon routing system," *IEEE Robot. Automat. Mag.*, vol. 22, no. 1, pp. 97–105, Mar. 2015.

[37] M. Li *et al.*, "An attention-controlled hand exoskeleton for the rehabilitation of finger extension and flexion using a rigid-soft combined mechanism," *Front. Neurorobot.*, vol. 13, 2019, Art. no. 34.

[38] A. Borboni, M. Mor, and R. Faglia, "Gloreha—Hand robotic rehabilitation: Design, mechanical model, and experiments," *J. Dyn. Syst. Meas. Control*, vol. 138, no. 11, 2016, Art. no. 111003.

[39] M. Dragusanu, T. Lisini Baldi, Z. Iqbal, D. Prattichizzo, and M. Malvezzi, "Design, development, and control of a tendon-actuated exoskeleton for wrist rehabilitation and training," in *Proc. IEEE Int. Conf. Robot. Autom.*, 2020, pp. 1749–1754.

[40] M. Malvezzi, T. Lisini Baldi, A. Villani, F. Ciccarese, and D. Prattichizzo, "Design, development, and preliminary evaluation of a highly wearable exoskeleton," in *Proc. IEEE Int. Symp. Robot Hum. Interactive Commun.*2020, pp. 1055–1062.

[41] M. Dragusanu, T. Lisini Baldi, Z. Iqbal, D. Prattichizzo, and M. Malvezzi, "Design, development and control of a tendon-actuated exoskeleton for wrist rehabilitation and training," in *Proc. IEEE Int. Conf. Robot. Automat.*, 2020, pp. 1749–1754.

[42] F. J. Valero-Cuevas, M. E. Johanson, and J. D. Towles, "Towards a realistic biomechanical model of the thumb: The choice of kinematic description may be more critical than the solution method or the variability/uncertainty of musculoskeletal parameters," *J. Biomech.*, vol. 36, no. 7, pp. 1019–1030, 2003.

[43] M. Santello, M. Flanders, and J. F. Soechting, "Postural hand synergies for tool use," *J. Neurosci.*, vol. 18, no. 23, pp. 10105–10115, 1998.
[44] M. Dragusanu, Z. Iqbal, D. Prattichizzo, and M. Malvezzi, "Design of a modular hand exoskeleton for rehabilitation and training," in *Proc. ASME Int. Mech. Eng. Congr. Expo.*, 2021, vol. 85598, Art. no. V005T05A067.
[45] T. Lisini Baldi, F. Farina, A. Garulli, A. Giannitrapani, and D. Prattichizzo, "Upper body pose estimation using wearable inertial sensors and multiplicative Kalman filter," *IEEE Sensors J.*, vol. 20, no. 1, pp. 492–500, Jan. 2020.
[46] T. R. Kratochwill *et al.*, "Single-Case Designs Technical Documentation," *What Works Clearinghouse*, Washington, DC, USA, 2010.
[47] D. Ao, R. Song, and J. Gao, "Movement performance of human-robot cooperation control based on EMG-driven hill-type and proportional models for an ankle power-assist exoskeleton robot," *IEEE Trans. Neural Syst. Rehabil. Eng.*, vol. 25, no. 8, pp. 1125–1134, Aug. 2017.

Mihai Dragusanu (Graduate Member, IEEE) received the M.Sc. degree in computer and automation engineering in 2018 from the Department of Information Engineering and Mathematics, University of Siena, Siena, Italy with the maximum score (110/110 cum laude) discussing a thesis on the design of a wrist exoskeleton for rehabilitation applications. He is currently working toward the Ph.D. degree in information engineering with the University of Siena, Siena, Italy.

His research activities focus on the design, prototyping, testing, and control of wearable devices for applications in rehabilitation and haptics.

Muhammad Zubair Iqbal (Member, IEEE) received the B.E. degree in mechatronics engineering in 2010 and the M.Sc. degree in mechanical engineering in 2016 from the National University of Science and Technology Pakistan, Islamabad, Pakistan, and the Ph.D. degree in robotic and automation in 2021 from the Department of Information Engineering and Mathematics, University of Siena, Siena, Italy.

His research interests include robotics and haptics focusing on supernumerary limbs, rehabilitation robotics, and industrial soft rigid grippers.

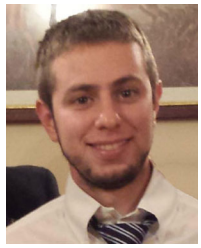

Tommaso Lisini Baldi (Member, IEEE) received the M.Sc. degree (*cum laude*) in computer and automation engineering and the Ph.D. degree in robotic and automation in 2014 and 2018, respectively, from the Department of Information Engineering and Mathematics, University of Siena, Siena, Italy.

He was a Ph.D. fellow with the Department of Advanced Robotics, Istituto Italiano di Tecnologia, from 2014 to 2017. His research interests include robotics and haptics focusing on hand tracking, haptics feedback, and motion tracking with inertial sensors.

Domenico Prattichizzo (Fellow, IEEE) received the M.S. degree in electronics engineering and the Ph.D. degree in robotics and automation from the University of Pisa, Pisa, Italy, in 1991 and 1995, respectively.

He is a Professor of robotics with the University of Siena, Siena, Italy, and since 2009, a Scientific Consultant with Istituto Italiano di Tecnoloogia, Genova, Italy. In 1994, he was a visiting scientist with the MIT AI Lab. He has authored more than 200 papers in his research fields. His main research interests include haptics, grasping, visual servoing, mobile robotics, and geometric control.

Dr. Prattichizzo has been the Chair of the IEEE RAS Early Career Awards Evaluation Panel since 2013. He was the Vice Chair for the special issues of the IEEE Technical Committee on Haptics during 2006–2010. He was the Chair of the Italian Chapter of the IEEE RAS during 2006–2010. He was a recipient of the IEEE 2009 Chapter of the Year Award. He is the Leader of a research unit in several EU projects. He is also the Coordinator of an EU ECHORD-EXPERIMENT and an EU IP collaborative project.

Monica Malvezzi (Member, IEEE) received the Laurea degree in mechanical engineering from the University of Florence, Florence, Italy, in 1999 and the Ph.D. degree in applied mechanics from the University of Bologna, Bologna, Italy, in 2003.

From 2002 to 2008, she was a Researcher with the Department of Energy, University of Florence. From 2008 to 2018, she was an Assistant Professor of mechanics and mechanism theory with the Department of Information Engineering and Mathematics, University of Siena, Siena, Italy, where since 2018, she has been an Associate Professor. She was a visiting scientist with Istituto Italiano di Tecnologia, IIT, Genova, Italy, from 2015 to 2019. Her main research interests include control of mechanical and mechatronic systems, robotics, haptics, vehicle localization, multibody dynamics, and grasping and dexterous manipulation.